Bioprocess Biosyst Eng (2015) 38:155–163
DOI 10.1007/s00449-014-1254-x

ORIGINAL PAPER

Zinc oxide quantum dots: a potential candidate to detain liver cancer cells

Javed Ahmad · Rizwan Wahab · Maqsood A. Siddiqui · Javed Musarrat · Abdulaziz A. Al-Khedhairy

Received: 25 April 2014 / Accepted: 3 July 2014 / Published online: 30 July 2014

Abstract The term cancer is used for diseases in which abnormal cells proliferate without control and are able to attack with other tissues. Over various types of cancers, liver cancer is the most hurtful disease, which affects the whole body system. The aim of the present study was to investigate the efficiency against cancer cells of HepG2 cells, with quantum dots of ZnO. The cytotoxic effects were analyzed with MTT assays in range of 1–100 μg/ml. The cells were exposed to ZnO-QDs and it exhibit significant reduction, which starts from concentration 5 μg/ml (4 %; $p < 0.05$). The assay was justified with quantitaive RT-PCR and it demonstrates, exposure of ZnO-QDs on HepG2 cells. The level of mRNA expressions was significantly up-regulated (Bax, P53, and Caspase-3), whereas the anti-apoptotic gene (Bcl-2) was down-regulated. The QDs (5 ± 2 nm) were prepared via soft chemical solution process and analyzed using FESEM, TEM and HR-TEM.

Keywords Quantum dots · HepG2 cells · FESEM · TEM · Apoptosis

J. Ahmad (✉) · R. Wahab (✉) · M. A. Siddiqui · A. A. Al-Khedhairy
Department of Zoology, College of Science, King Saud University, P.O. Box 2455, Riyadh 11451, Saudi Arabia
e-mail: javedahmad@ksu.edu.sa

R. Wahab
e-mail: rwahab@ksu.edu.sa

J. Ahmad · R. Wahab · M. A. Siddiqui · A. A. Al-Khedhairy
Department of Zoology, College of Science, King Saud University, P.O. Box 2455, Riyadh 11451, Saudi Arabia

J. Musarrat
Department of Agricultural Microbiology, Faculty of Agricultural Sciences, Aligarh Muslim University, Aligarh 202002, UP, India

Introduction

Cancer is not only one disease, its a collection of many disease, which is caused due to cellular disorder. The cellular disorder happens in the body either by natural mutation or through apoptosis. Till date, over more than 100 different types of cancers are observed. Mostly, cancers are named for the organ or type of cell, from where they start for example, cancer that begins in melanocytes of the skin is called melanoma. Over various types of cancers, hepatocellular carcinoma is the fourth most common malignant tumor in the world [1, 2]. Usually, lung cancer is prevalent in many countries such as the United States, United Kingdom, Japan and China. With an estimated average of 0.5–1 million cases diagnosed every year worldwide, it accounts for 5.6 % of all human cancers, with 7.5 % among men and 3.5 % among women. This disease generally affects the developing countries and has a greater share of burden to the leading cause of cancer incidence and mortality among males [3–7]. Hepatocellular carcinoma (HCC) and cholangio carcinoma are the two major types, which accounting for 85 and 10 % of all primary liver cancers, respectively [4–7]. Approximately 81 % of all HCC cases are found in Asia and Africa, with China producing 53 % of these cases. The disease affects at the age of 20 at high risk, whereas typically stabilized at age of 50 and older [4–7]. The most common failure of hepatic is the chronic hepatitis or alcoholic liver disease, which ends in the form of cirrhosis. Mostly (about 85 %), the patients are infected chronically with hepatitis B virus (HBV) which develops cirrhosis [4–8]. Therapies such as, chemotherapy, radiotherapy, immune therapy have been adopted to protect cancer but the outcome rate is remains negligible [9–11]. Recently, the combined efforts of nanotechnology and nano-biotechnology are largely used

to protect cancers because, the treatments of cancers are very expensive and are limited to therapies. The inexpensive nanoscale materials, which exhibit unique physico-chemical characteristic due to their size, surface area, enhanced reactivity can easily enter in cells, protein and hence it can effectively participate for cancer diagnosis, treatment, and prevention [9–11]. Among various types of metal oxide nanostructures, prepared either by physical or chemical methods such as chemical vapor deposition (CVD), spray pyrolysis, ion beam assisted deposition, laser-ablation, sputter deposition, flame transport approach, template assisted growth, solution route, sol–gel, wet chemical and non-aqueous methods [12–16]. ZnO nanostructures possess excellent properties and wide applications. Due to their excellent properties of ZnO, such as wide band gap, high-exciton energy, low-cost synthesis, high-specific surface area, high conductivity, bio-compatibility nature and so on, it is widely used for variety of applications, to name a few, photocatalysis, sun-screen, cosmetic products, optoelectronic devices, solar cells, chemical, bio and gas sensors, piezoelectric devices, light emitting diodes, several biological applications such as antibacterial, antifungal agents [10, 17–23]. Towards this direction several application related to cytotoxic studies had been performed such as nano and micro structure of ZnO, immitiates filopodia cells and can target in HSV-1 pathogenesis [24]. The nanostructures of zinc oxide tetra pod like structures also have the ability to block the entry and spread of HSV-2 virus into target cells [25] and can neutralize HSV-2 virions [25]. In another report, the cellular mechanism and dissolved Zn^{2+} ions had been investigated in presence of tetrapods like structure of ZnO [26]. Over various applications of nano and micro structures of ZnO, the utilization of quantum dots is still in primary phase towards cancer prevention. Here, we have investigated the cytotoxicity against HepG2 cells using well characterized ZnO-QDs because the used cell line was largely employed for the toxicities studies. Here, we have also checked the detailed characterization of the materials.

Materials and methods

Fabrication of ZnO-QDs

The fabrication of zinc oxide QDs was performed using zinc nitrate hexahydrate ($Zn(NO_3)_2{\cdot}6H_2O$), *n*-propyl amine and surfactant CTAB (cetyl trimethyl ammonium bromide). In a typical experiment: $Zn(NO_3)_2{\cdot}6H_2O$ (0.3 M) and *n*-propyl amine were dissolved in 100 ml of methanol (MeOH) under continuous stirring at room temperature. To this solution, 5 mg of surfactant of CTAB was mixed and the solution was again stirred for 30 min for to complete

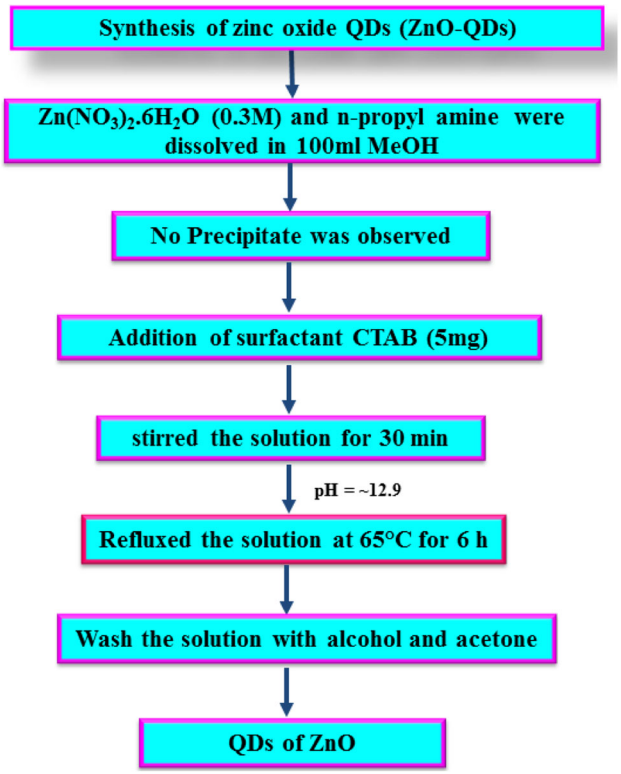

Fig. 1 Flow chart for the formation of zinc oxide QDs

dissolution. The pH of the prepared solution was measured and it was reached upto 12.9. After the dissolution of mixture, solution was transferred to the refluxing pot and refluxed at ~65 °C for 6 h. The formed white powder of ZnO-QDs was washed several time with alcohols such as methanol, ethanol and acetone to remove the ionic impurities and dried at room temperature (as described in flow chart for the formation of ZnO-QDs, Fig. 1). The obtained dried white powder sample was characterized in terms of their morphological and chemical properties.

Characterization of ZnO-QDs

The obtained QDs were characterized with the standard characterization tools such as the morphology of the grown QDs were analyzed via field emission electron microscopy (FESEM), whereas further confirmation of morphology and crystallinity were observed from transmission electron microscopy (TEM) equipped with HR-TEM. For the observation of FESEM (JEOL-JSM-7600F, Japan) powder of grown QDs were uniformly sprayed on carbon tape and coated with thin osmium oxide (OsO_4) for 5 s. Further, the morphology was again justified with TEM, for TEM (Jeol JSM-2010, Japan) measurement, powder was sonicated in an alcohol ethanol for 10 min and then a carbon coated copper grid (400 mesh) was dipped to this dispersion

solution and dried at room temperature. The dried copper grid was fixed in a sample holder and analyzed at 200 kV.

Cell culture

The liver cancer cells HepG2 were cultured in DMEM/MEM medium supplemented with 10 % fetal bovine serum (FBS), 0.2 % sodium bicarbonate, and antibiotic–antimycotic solution (100×, 1 ml/100 ml of medium). The cells were grown in a humidified environment 5 % CO_2 and 95 % atmosphere at 37 °C. Prior to use in the experiments, cells were assessed for cell viability by trypan blue dye exclusion assay following the protocol of and batches [27] showing viability more than 95 % were only used in the study. HepG2 cells were used between passages 10–12 to treat the cells with QDs.

Reagents and consumables

The MTT [3-(4,5-dimethylthiazol-2-yl)-2,5 diphenyltetrazolium bromide] and all the specified chemicals were purchased from Sigma Aldrich Chemical Corporation Pvt. Ltd., USA. DMEM and MEM culture medium, antibiotics–antimycotic solution and FBS were purchased from Invitrogen, USA. Culture wares and other plastic consumables used in the study were procured commercially from Nunc, Denmark.

MTT assay

The Percent cell viability was assessed using the MTT assay with the following protocol [28]. In brief, cells (1×10^4) were seeded in 96 well culture plates and allowed to adhere for 24 h under high humid environment in 5 % CO_2 and 95 % O_2 atmosphere at 37 °C. Then cells were exposed to various concentrations (1, 2, 5, 10 and 25 µg/ml) of QDs for 24 h. After the exposure, MTT (5 mg/ml of stock in PBS) was added 10 µl/well in 100 µl of cell suspension and plate were incubated for 4 h. At the end of incubation period, the reaction mixture was carefully taken out and 200 µl of DMSO was added to each well and mixed gently. The plates were kept on rocker shaker for 10 min at room temperature and then read at 550 nm using multiwell micro plate reader (Multiskan Ex, Thermo Scientific, Finland). Untreated sets were also run under identical conditions and served as control.

Total RNA isolation and quantitative real-time PCR analysis of apoptotic markers

For isolation of total RNA, HepG2 cells were cultured in 6-well plates and exposed to ZnO-QDs at a concentration of 50 µg/ml for 24 h. At the end of exposure total RNA was extracted by RNeasy mini Kit (Qiagen) according to the manufacturer's instructions. Concentration of the extracted RNA was determined using Nanodrop 8000 spectro-photometer (Thermo-Scientific) and the integrity of RNA was visualized on 1 % agarose gel using gel documentation system (Universal Hood II, BioRad). The first strand cDNA was synthesized from the total RNA by Reverse Transcriptase using oligo-p(dT)12–18 primer and MLV Reverse Transcriptase (GE HealthCare, UK). The following sets of specific primers were employed for amplification of each cDNA: p53, caspase 3, Bax, BCl_2. Expression was normalized to HPRT gene expression, which was used as an internal housekeeping control. Real-time quantitative PCR (RT-PCRq) was performed by Quanti Tect SYBR Green PCR kit (Qiagen) using Light Cycler® 480 instrument with 96-well plate (Roche Diagnostics, Rotkreuz, Switzerland). The results were obtained from three subsamples and PCR was repeated twice per sample. Relative quantification analysis was performed by use of Roche LightCycler® 480 software Version 1.5. Expression of mRNA normalized to the HPRT gene was calculated, and the data were subjected to test to identify significant differences between cells treated with ZnO-QDs compared to untreated control.

Results and discussion

Morphological and crystalline studies of the prepared ZnO-QDs

The FESEM was used to observe the morphology of the QDs and presented in Fig. 2. Low (Fig. 2a) and high (Fig. 2b) magnified FESEM images show the spherical shaped structures of tiny, smooth and clear morphology of the grown QDs prepared at an above conditions. The QDs are in very high density, and exhibit very small diameter ($\sim 5 \pm 2$ nm). Further, general morphology of the grown structure was again elucidated in detail from TEM and the results are shown in Fig. 2c. The high resolution TEM (HR-TEM) image was captured from the white circle and presented in Fig. 2d of grown QDs. The lattice fringes between two adjacent planes are about 0.265 nm apart, which is equal to the lattice constant of wurtzite ZnO, which further indicates that the grown powder is pure ZnO. The high resolution picture is fully consistent with FESEM observation. The corresponding HR-TEM observation corresponds that the synthesized product is crystalline in nature [9].

Possible proposed mechanism for the formation of ZnO-QDs

The formation mechanism of ZnO-QDs in chemical solution can be understand with the help of using characterizations and obviously the used synthesis process as mentioned

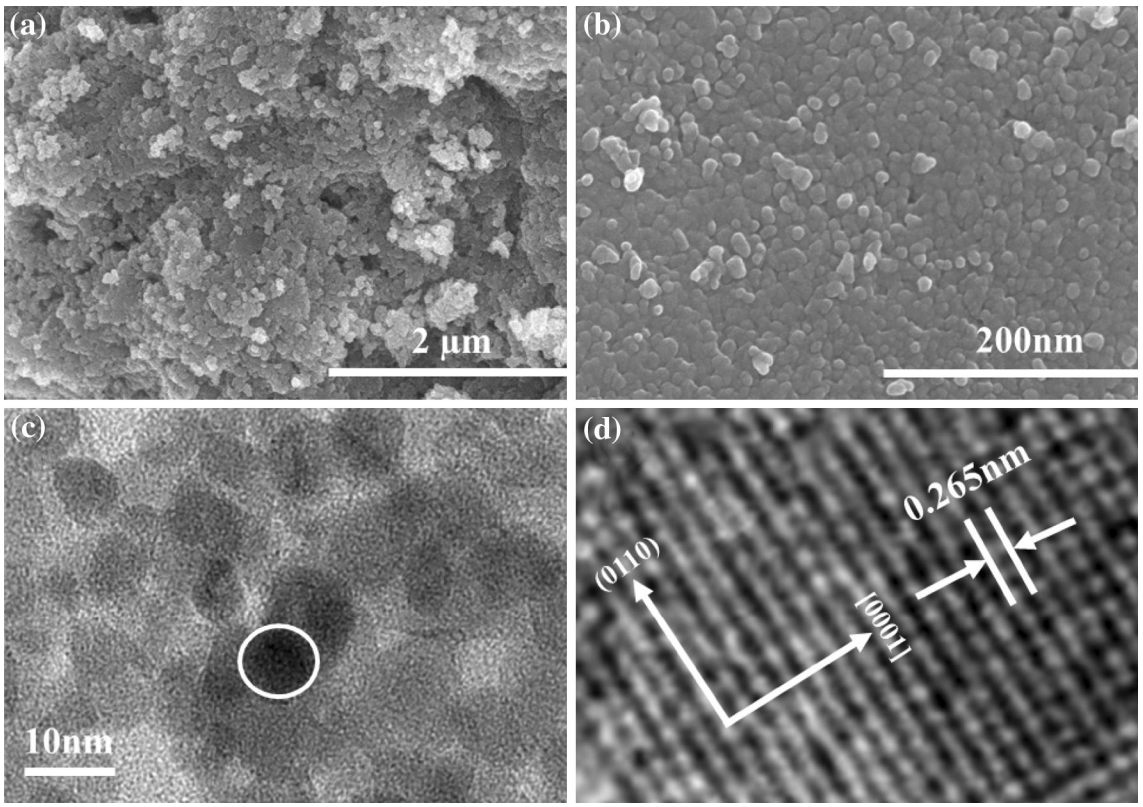

Fig. 2 Represents the low (**a**) and high (**b**) magnified field emission electron microscopic (FESEM) images whereas **c**, **d** shows the transmission electron microscopic (TEM) and high resolution transmission electron microscopic images (HR-TEM) of grown QDs, respectively. The *white circle* represents the HR-TEM image of grown particles, which shows the difference between two lattice fringes, which is about 0.265 nm (**d**)

above. Here, we have designed a proposed formation mechanism of ZnO-QDs using zinc nitrate hexahydrate, *n*-propylamine and CTAB with using methanol solvent medium and were refluxed for 6 h. The common liquid precipitation phenomenon describes that when metal salts, react with low soluble compound precipitate out of the reaction. The method has been extensively employed for the large-scale production of metal oxide powders. In this case, a simple chemical reaction between zinc nitrate hexahydrate ($Zn(NO_3)_2{\cdot}6H_2O$), *n*-propylamine and surfactant CTAB were exist. When zinc nitrate hexa hydrate ($Zn(NO_3)_2{\cdot}6H_2O$) was dissolved under continuous stirring in solution of *n*-propylamine with methanol (MeOH) solvent, it forms a clear solution without precipitate at pH ~12.7. To this solution ($Zn(NO_3)_2{\cdot}6H_2O$), *n*-propyl amine), small amount of surfactant CTAB (5 mg) of CTAB was mixed, small fluctuation of pH was observed to 12.9. The solution turn in soapy liquid and were transferred to the refluxing pot and heated for 6 h at ~65 °C. Initially, no precipitate was formed but as the refluxing temperature rises, a white precipitate started to form and it was completed in 6 h. It is assumed from the solution that the nitrate (NO_3^-) group from zinc nitrate decomposes during heating and when the refluxing increases in solvent methanol (CH_3OH), it reacts with hydrogen ions (H^+ ions) of propylamine and forms zinc complex ($ZnN–(CH_2)–CH_3$) (Eq. 1). The formed complex further reacts with the solvent methanol and the product zinc hydroxide and by product formed as reaction 2 (Eq. 2).

$$Zn\begin{matrix}NO_3\\ .6H_2O\\ NO_3\end{matrix}\begin{matrix}H\\ +\\ H\end{matrix}N\text{-}(H_2C)\text{-}CH_3 \xrightarrow[-2HNO_3]{2CH_3OH} Zn\ N\text{-}(CH_2)\text{-}CH_3 + 6H_2O \quad (1)$$

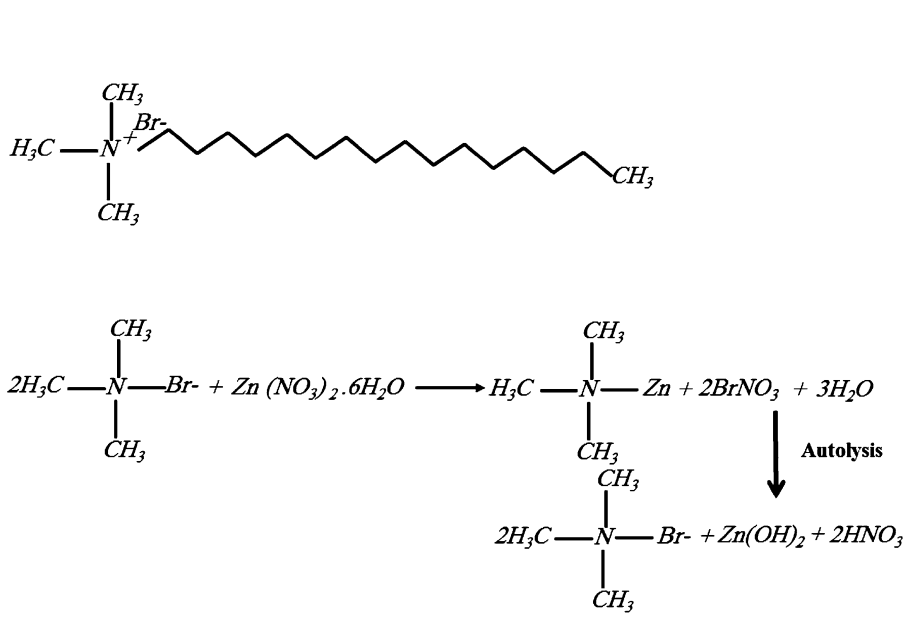

(2)

(3)

(4)

$$Zn(OH)_2 \longrightarrow ZnO + H_2O \quad (5)$$

The brominated chain of surfactant CTAB (Eq. 3) was reacted with zinc nitrate hexahydrate solution and further it changes into the methylated complex [$(CH_3)_3NZn$)], bromine nitrate ($BrNO_3$) and water molecule (Eq. 4), which further autolysed. As the refluxing temperature and time rises, the hydroxide molecule of zinc hydroxide ($Zn(OH)_2$) changes to zinc oxide (ZnO) and water molecules (Eq. 5). The formed organic by products from the reaction were leached out during centrifugation of the product and pure zinc oxide quantum dots were formed. The possible proposed chemical mechanism analogous with the previous publications [9, 18, 19].

Quantum dots-induced cytotoxicity (MTT assay)

The Yellow MTT (3-(4,5-dimethylthiazol-2-yl)-2,5-di phenyltetrazolium bromide, a tetrazole) solution was used to determine viability of the cells, which leads to mitochondrial dysfunction and therefore decreased performance in the assay. This mostly happens in mitochondria, and the assays are therefore largely measured for mitochondrial activity [29]. The MTT is reduced into purple formazan salt in the mitochondria of living cells. The absorbance of colored solution was quantified by spectrophotometer at a certain wavelength (usually ~550–570 nm). The absorption maximum was depending upon the solvent employed and the level of percentage (%) viability was calculated according to the equations mentioned below:

$$\% \text{ Viability} = [(\text{total cells} - \text{viable cells})/\text{total cells}] \times 100$$

or

$$\% \text{ Viability} = \text{OD (optical densities) in sample well/OD in control well} \times 100$$

HepG2 cells were exposed to ZnO-QDs (1, 2, 5, 10 and 25 lg/ml) for 24 h. The cytotoxicity was measured by MTT assays. The obtained result shows that cell viability was reduced by ZnO-QDs and degree of reduction was conc entration/dose-dependent (Fig. 3). No adverse effect was observed at very low concentration of QDs such as 1 and 2 lg/ml but as the concentration was increased to 5–100 lg/ml, significant changes has been observed. The HepG2

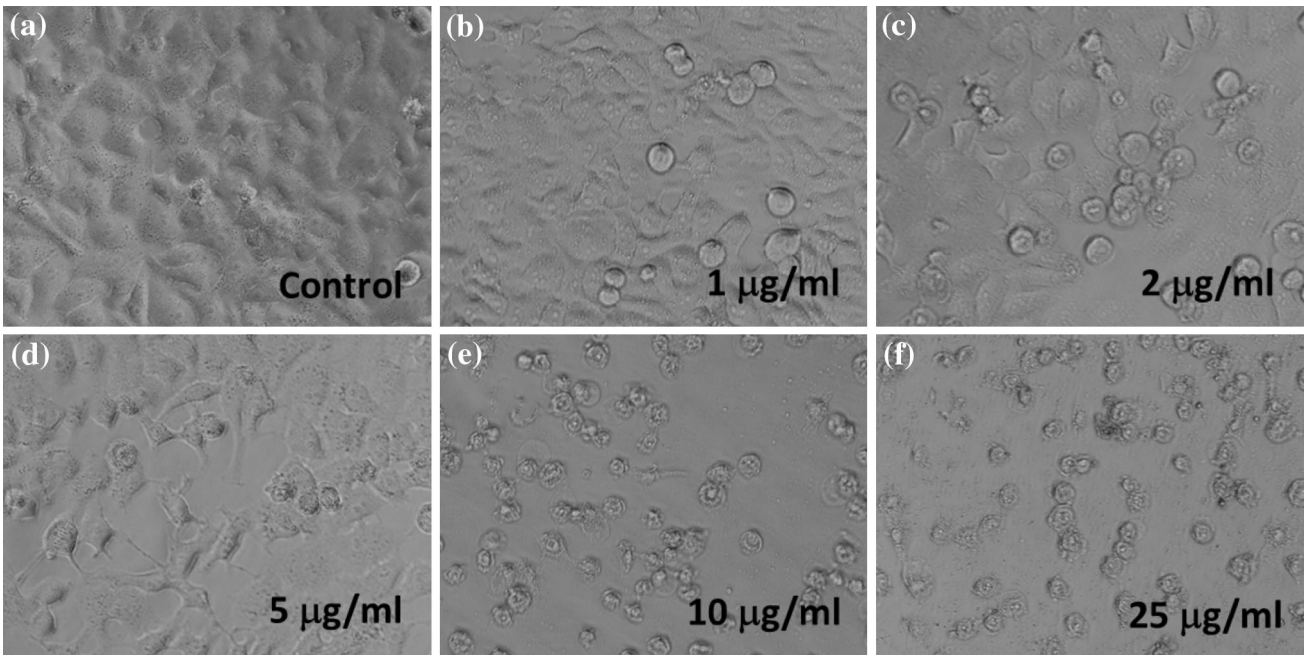

Fig. 3 Morphological changes in HepG2 cells exposed to zinc oxide nanoparticles for 24 h

Fig. 4 Cytotoxicity assessment by MTT assay in HepG2 cells exposed to QDs of ZnO for 24 h

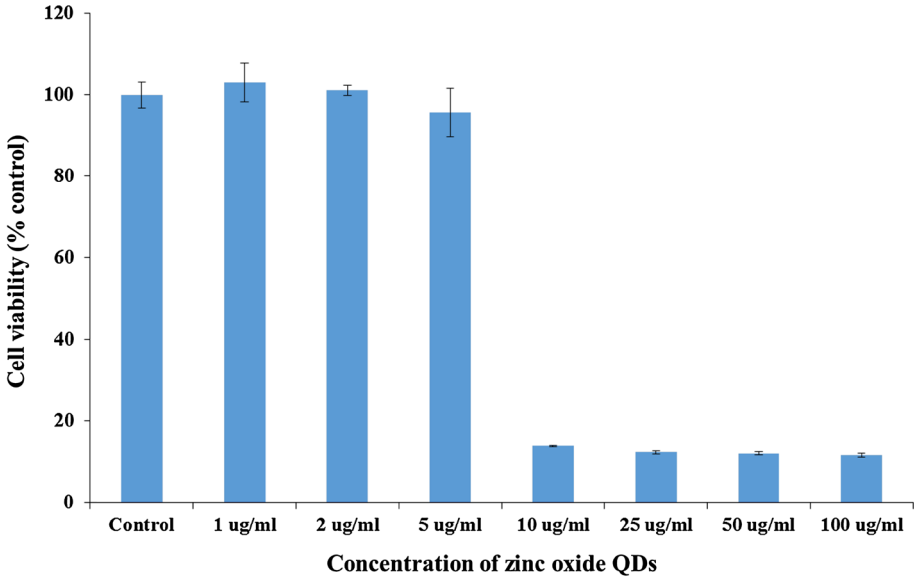

cells were damaged at 24 h incubation are 4, 86, 87, 88, 88 % (Fig. 4) for the concentrations of 5, 10 and 25 and 100 lg/ml, respectively ($p < 0.05$ for each). The HepG2 cells were also exposed to ZnO-QDs (1–100 lg/ml) for 24 h for NRU assay. Results show that the cells damage by QDs was consistent with MTT assay and degree of reduction was dose dependent. In NRU assay reduction was 16, 81, 82, 83 and 84 % for the concentrations of 5, 10, 25, 50 and 100 lg/ml, respectively ($p < 0.05$ for each) (Fig. 5). No significant change was observed at a very low concentration of ZnO-QDs.

Quantitative real-time PCR results

The quantitative real-time PCR was utilized to analyze the mRNA levels of apoptotic markers (e.g. p53, bcl-2, bax, and caspase-3) in HepG2 cells exposed to ZnO-QDs at a concentration of 50 µg/ml for 24 h. Results showed that the mRNA levels of these apoptotic markers were significantly altered in HepG2 cells due to ZnO-QDs exposure (Fig. 6, $p < 0.05$ for each). The mRNA level of tumor suppression gene p53 was 1.7-fold higher whereas in anti-apoptotic gene bcl-2 (0.25-fold) it was lower and

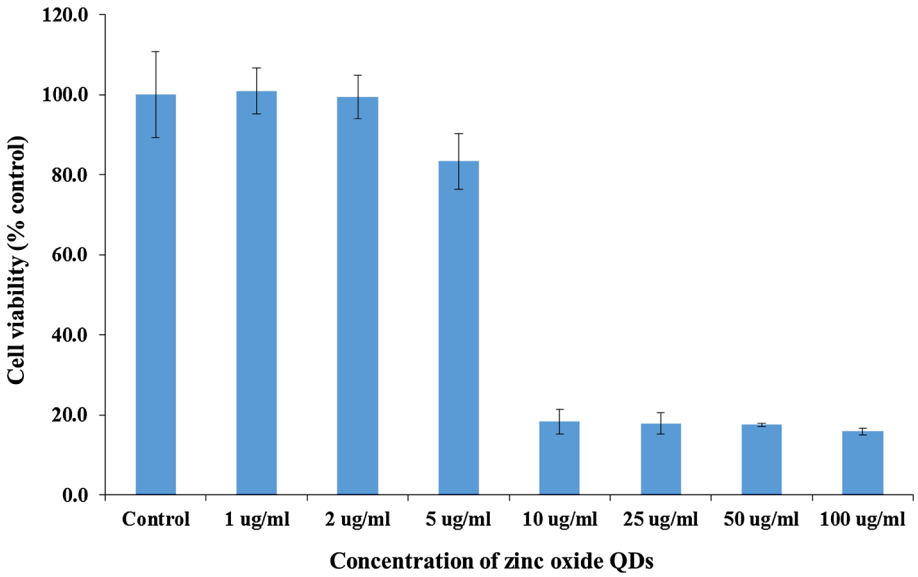

Fig. 5 Cytotoxicity assessment by NRU assay in HepG2 cells exposed to QDs of ZnO for 24 h

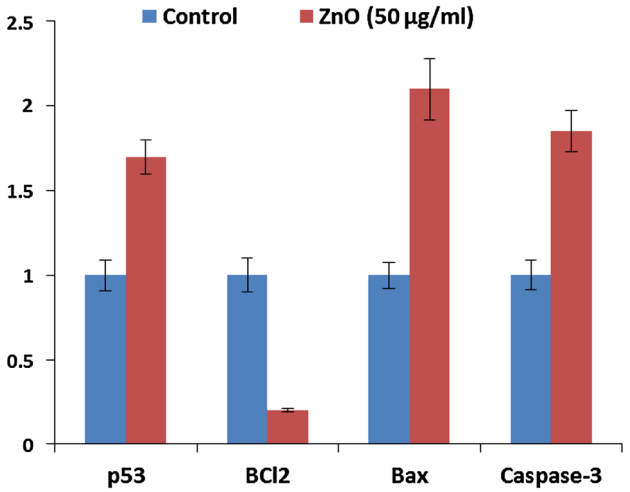

Fig. 6 Effect of ZnO-QDs on mRNA expression level of apoptotic markers in HepG2 cells. Cells were treated with QDs of zinc oxide at a concentration of 50 µg/ml for 24 h. Quantitative real-time PCR was performed by use of a Roche LightCycler® 480 software Version 1.5. HPRT gene was calculated as the internal control to normalize the data. Data represented are mean ± SD of three identical experiments made in three replicate. *Asterisk* statistically significant difference as compared to the controls ($p < 0.05$ for each)

expression (Fig. 6) in exposed cells than those of untreated cells, while mRNA expression of pro-apoptotic gene bax (2.2-fold) (Fig. 6). Moreover, we examined the effect of ZnO-QDs on the mRNA expression of caspase-3 was 1.9-fold higher in treated cells in comparison with untreated control cells (Fig. 6). We analyzed the mRNA expression of genes; p53, bcl-2, bax, and caspase in response to ZnO-QDs exposure in HepG2 cells, because apoptosis is controlled through these pathways. Quantitative real-time PCR results showed that ZnO-QDs up-regulated mRNA level of cell cycle checkpoint protein p53 and pro-apoptotic protein bax. Expression of anti-apoptotic proteins bcl-2 was down-regulated in cells exposed to ZnO-QDs. Furthermore, together, up-regulation of p53 and down-regulation of bcl-2 family, such as bax induces permeabilization of the outer mitochondrial membrane, which releases soluble proteins from the intermembrane space into the cytosol, where they promote caspase activation [30, 31].

Possible proposed mechanism of ZnO-QDs with liver cancer cells

On the basis of chemical and biological result and their observations, we may assume that the role of small QDs acts as anticancer nanodrug against liver cancer of HepG2. The QD/nanoparticles cytotoxicity depends on a variety of physicochemical properties such as size, shape, chemical structure, and surface coating of the nano particles and it also possible that the cytotoxicity of nanoparticles could affect the endocytic uptake of cells [32]. The spherical-shaped ZnO-QDs were introduced to the cancer cells at dose-dependent (1–100 µm/ml) manner and incubated at 24 h. It is postulated that QDs first attacked on outer membrane and penetrate the outer layer of cancer cells. The cells have small pores which helps, the QDs to enter into the inner membrane of cancer cells. The prepared QDs have property to enter into cells (~20 µm) very easily due to very small size (~5 ± 2 nm) as compared to the cells [32, 33]. The high density of small QDs in the liquid system strongly favors the rapid formation of agglomerates and it's assumed that these agglomerates of ZnO-QDs destroy the cell organelle such as DNA, RNA, endoplasmic reticulum, mitochondria [34, 35]. The ROS is a major factor, which is produced in aquaculture of cancer cells with QDs and are responsible to form the free radicals in the solution and

these free radicals are responsible to penetrate the outer wall of the cells and enter in to inner wall of the membrane. These free radicals when reacts with the organelles, enzymatic changes occurred and it leads to the disorganization of the cells and cell contents. The interaction of QDs/NPs with cancer cells and their extreme generation of ROS through QDs/NPs reduces the cellular antioxidant capacity production. The phenomena why ZnO-QDs are responsible to regulate the growth or destroy the cell organelles and their biochemical and enzymatic changes of cancer cells is under investigation and it needs further study to investigate the role of ZnO-QDs against HepG2 cancer cells [34, 35]. Most of the toxicity studies had been performed with metal oxide nanostructures at high concentration, which may be difficult for human exposure. We believe that the use of QDs of ZnO, which is a biocompatible and non-toxic material and at lower concentration would be helpful to control the growth cancer cells and have no adverse effect on the body [36].

Conclusions

In summary, the present study reveals that the prepared quantum dots behave as nanodrugs and are very effective at low concentration of QDs on HepG2 cells. The obtained results of antiproliferative studies are much dose dependent manner are sensitize to cancer cells. The apoptosis enhances with the increase of concentration of QDs. The cell death due to QDs was escorted by a significant increase in concentration. The detailed investigations and molecular mechanism could be helpful in designing more potent anticancer agents for the therapeutic use. The results of our study demonstrated that ZnO-QDs induce cytotoxicity and apoptosis in HepG2 cancer cells, which is likely to be mediated through ROS generation. The mechanisms against cytotoxicity with ZnO-QDs should be further investigated. The synthesis was designed with a simple and effective method to prepare high quality ZnO-QDs at a very low temperature. The characterization supports that the resultant materials present the formation of good quality QDs.

Acknowledgments JM is grateful to the visiting professor program (VPP) of the King Saud University, Riyadh, SA for all the help and support in conducting this collaborative research work.

References

1. American Cancer Society, Cancer Facts and Figures (2010) American Cancer Society, Atlanta GA. http://www.cancer.org/research/cancerfactsstatistics/cancerfactsfigures2010/index
2. Singh R, Nalwa HS (2011) Medical applications of nanoparticles in biological imaging, cell labeling, anti-microbial agents, and anticancer nanodrugs. J Biomed Nanotechnol 7:489–503
3. Anthony PP (2001) Hepatocellular carcinoma: an overview. Histopathology 39:109–118
4. Bosch FX, Ribes J, Cléries R, Diaz M (2005) Epidemiology of hepatocellular carcinoma. Clin Liver Dis 9(2):191–211
5. Yu MC, Yuan JM, Govindarajan S, Ross RK (2000) Epidemiology of hepatocellular carcinoma. Can J Gastroenterol 14(8):703–709
6. Aguayo A, Platt YZ (2001) Liver cancer. Clin Liver Dis 5(2):479–507
7. Marrero JA (2006) Hepatocellular carcinoma. Curr Opin Gastroenterol 22:248–253
8. Anderson MD (2006) Liver Tumor Study Group, (http://www.mdanderson.org/departments/LTSG/)
9. Wahab R, Dwivedi S, Umar A, Singh S, Hwang IH, Shin HS, Musarrat J, Al-Khedhairy AA, Kim YS (2013) ZnO nanoparticles induce oxidative stress in Cloudman S91 melanoma cancer cells. J Biomed Nanotechnol 9:441–449
10. Wahab R, Kaushik NK, Kaushik N, Choi EH, Umar A, Dwivedi S, Musarrat J, Al-Khedhairy AA (2013) ZnO nanoparticles induces cell death in malignant human T98G Gliomas, KB and non-malignant HEK Cells. J Biomed Nanotechnol 9:1181–1189
11. Siddiqui MA, Ahamed M, Ahmad J, Khan MAM, Musarrat J, Al-Khedhairy AA, Alrokayan SA (2012) Nickel oxide nanoparticles induce cytotoxicity, oxidative stress and apoptosis in cultured human cells that is abrogated by the dietary antioxidant curcumin. Food Chem Toxicol 50:641–647
12. Zahang H, Yang D, Li D, Ma X, Li S, Que D (2005) Controllable growth of ZnO micro crystals by a capping-molecule-assisted hydrothermal process. J Cryst Growth Des 5(2):547–550
13. Studenikin SA, Golego N, Cocivera M (1998) Fabrication of green and orange photoluminescent, undoped ZnO films using spray pyrolysis. J Appl Phys 84:2287–2294
14. Li W, Mao DS, Zheng ZH, Wang X, Liu XH, Zhu SC, Li Q, Xu JF (2000) ZnO/Zn phosphor thin films prepared by IBED. Surf Coat Technol 128:346–350
15. Sun Y, Fuge GM, Ashfold MNR (2004) Growth of aligned ZnO nanorod arrays by catalyst-free pulsed laser deposition methods. Chem Phys Lett 396:21–26
16. Mishra YK, Kaps S, Schuchardt A, Paulowicz I, Jin X, Gedamu D, Freitag S, Claus M, Wille S, Kovalev A, Gorb SN, Adelung R (2013) Fabrication of macroscopically flexible and highly porous 3D semiconductor networks from interpenetrating nanostructures by a simple flame transport approach. Part Part Syst Charact 30:775–783
17. Alem S, Lu J, Movileanu R, Kololuoma T, Dadvand A, Tao Y (2014) Solution-processed annealing-free ZnO nanoparticles for stable inverted organic solar cells. Org Electron 15(5):1035–1042
18. Wahab R, Tripathy SK, Shin HS, Mohapatra M, Musarrat J, Al-Khedhairy AA, Kaushik NK (2013) Photocatalytic oxidation of acetaldehyde with ZnO-quantum dots. Chem Eng J 226:154–160
19. Wahab R, Hwang IH, Kim YS, Shin HS (2011) Photocatalytic activity of zinc oxide micro-flowers synthesized via solution method. Chem Eng J 168:359–366
20. Wahab R, Hwang IH, Kim YS, Musarrat J, Siddiqui MA, Seo HK, Tripathy SK, Shin HS (2011) Non-hydrolytic synthesis and photo-catalytic studies of ZnO nanoparticles. Chem Eng J 175:450–457
21. Ansari SG, Ansari ZA, Wahab R, Kim YS, Khang G, Shin HS (2008) Glucose sensor based on nano-baskets of tin oxide templated in porous alumina by plasma enhanced CVD. Biosens Bioelectron 23(12):1838–1842
22. Wahab R, Kim YS, Hwang IH, Shin HS (2009) A non-aqueous synthesis, characterization of zinc oxide nanoparticles and their interaction with DNA. Synth Metals 159(23–24):2443–2452
23. Wahab R, Mishra A, Yun SIl, Hwang IH, Mussarat J, Al-Khedhairy AA, Kim YS, Shin HS (2012) Fabrication, growth

mechanism and antibacterial activity of micro-spheres prepared via solution process. Biomass Bioenergy 39:227–236
24. Mishra YK, Adelung R, Röhl C, Shukla D, Spors F, Tiwari V (2011) Virostatic potential of micro-nano filopodia-like ZnO structures against herpes simplex virus-1. Antiviral Res 92:305–312
25. Antoine TE, Mishra YK, Trigilio J, Tiwari V, Adelung R, Shukla D (2012) Prophylactic, therapeutic and neutralizing effects of zinc oxide tetrapod structures against herpes simplex virus type-2 infection. Antiviral Res 96:363–375
26. Papavlassopoulos H, Mishra YK, Kaps S, Paulowicz I, Abdelaziz R, Elbahri M, Maser E, Adelung R, Röhl C (2014) Toxicity of functional nano-micro zinc oxide tetrapods: impact of cell culture conditions, cellular age and material properties. PLoS One 9(1):e84983
27. Siddiqui MA, Kashyap MP, Kumar V, Al-Khedhairy AA, Musarrat J, Pant AB (2010) Protective potential of trans-resveratrol against 4-hydroxynonenal induced damage in PC12 cells. Toxicol In Vitro 24:1592–1598
28. Siddiqui MA, Singh G, Kashyap MP, Khanna VK, Yadav S, Chandra D, Pant AB (2008) Influence of cytotoxic doses of 4-hydroxynonenal on selected neurotransmitter receptors in PC-12 cells. Toxicol In Vitro 22:1681–1688
29. Mosmann T (1983) Rapid colorimetric assay for cellular growth and survival: application to proliferation and cytotoxicity assays. J Immunol Methods 65(1–2):55–63
30. Pablo FP, Guy SS (2004) The protein structures that shape caspase activity, specificity, activation and inhibition. Biochem J 384:201–232
31. Youle RJ, Strasser A (2008) The BCL-2 protein family: opposing activities that mediate cell death. Nat Rev Mol Cell Biol 9(1):47–59
32. Chang E, Thekkek N, Yu WW, Colvin VL, Drezek R (2006) Evaluation of quantum dot cytotoxicity based on intracellular uptake. Small 12:1412–1417
33. Limbach LK, Li Y, Grass RN, Brunner TJ, Hintermann MA, Muller M, Gunther D, Stark WJ (2005) Oxide nanoparticle uptake in human lung fibroblasts: effects of particle size, agglomeration, and diffusion at low concentrations. Environ Sci Technol 39(23):9370–9376
34. Ahamed M, AlSalhi MS, Siddiqui MKJ (2010) Silver nanoparticle applications and human health. Clin Chim Acta 411:1841–1848
35. Wise JP, Goodale BC, Wise SS (2010) Silver nanospheres are cytotoxic and genotoxic to fish cells. Aquat Toxicol 97:34–41
36. Hussain SM, Schlager JJ (2009) Safety evaluation of silver nanoparticles: inhalation model for chronic exposure. Toxicol Sci 108:223–224